Expectation and dyspnoea: the neurobiological basis of respiratory nocebo effects

Elke Vlemincx [1,2], Christian Sprenger [1,3] and Christian Büchel [1]

[1]Dept of Systems Neuroscience, University Medical Center Hamburg-Eppendorf, Hamburg, Germany. [2]Dept of Health Sciences, VU University Amsterdam, Amsterdam, The Netherlands. [3]Dept of Anesthesiology, University Medical Center Hamburg-Eppendorf, Hamburg, Germany.

Corresponding author: Elke Vlemincx (e.vlemincx@vu.nl)

Shareable abstract (@ERSpublications)
A neural dyspnoea nocebo effect was found; expectations of dyspnoea increase the central neural processing of dyspnoea and respiratory effort as seen by activation of the periaqueductal gray and deactivation of the rostral anterior cingulate cortex http://bit.ly/3p2TsA6

Cite this article as: Vlemincx E, Sprenger C, Büchel C. Expectation and dyspnoea: the neurobiological basis of respiratory nocebo effects. *Eur Respir J* 2021; 58: 2003008 [DOI: 10.1183/13993003.03008-2020].

This article has supplementary material available from erj.ersjournals.com

This article has an editorial commentary: https://doi.org/10.1183/13993003.01876-2021

Received: 18 Jan 2019
Accepted: 31 Jan 2021

Abstract

Cues such as odours that do not *per se* evoke bronchoconstriction can become triggers of asthma exacerbations. Despite its clinical significance, the neural basis of this respiratory nocebo effect is unknown.

We investigated this effect in a functional magnetic resonance imaging (fMRI) study involving 36 healthy volunteers. The experiment consisted of an experience phase in which volunteers experienced dyspnoea while being exposed to an odorous gas ("Histarinol"). Volunteers were told that Histarinol induces dyspnoea by bronchoconstriction. This was compared with another odorous gas which did not evoke dyspnoea. Dyspnoea was actually induced by a concealed, resistive load inserted into the breathing system. In a second, expectation phase, Histarinol and the control gas were both followed by an identical, very mild load. Respiration parameters were continuously recorded and participants rated dyspnoea intensity after each trial.

Dyspnoea ratings were significantly higher in Histarinol compared with control conditions, both in the experience and in the expectation phase, despite identical physical resistance in the expectation phase. Insula fMRI signal matched the actual load, *i.e.* a significant difference between Histarinol and control in the experience phase, but no difference in the expectation phase. The periaqueductal gray showed a significantly higher fMRI signal during the expectation of dyspnoea. Finally, Histarinol-related deactivations during the expectation phase in the rostral anterior cingulate cortex mirrored similar responses for nocebo effects in pain.

These findings highlight the neural basis of expectation effects associated with dyspnoea, which has important consequences for our understanding of the perception of respiratory symptoms.

Introduction

Contextual information dramatically shapes the perception of symptoms and is therefore critical in all disease states. Recent theoretical accounts of symptom perception have explained interoception to result from specific internal sensations, such as sensations of pain or airway resistance, as well as expectations, often resulting from prior experience [1–3]. This Bayesian framework can account for placebo and nocebo effects, in which symptom improvement and symptom worsening, respectively, in response to an inert treatment are caused by expectations attributed to aspects of the treatment. Evidence for placebo effects in the domain of pain has been established repeatedly [4] and evidence for nocebo effects in pain is growing [5, 6]. However, findings on placebo and nocebo effects in the respiratory system are scarce [7, 8].

In asthma patients, placebo treatment significantly improved asthma symptoms but did not change physiological parameters of lung function [7, 9, 10]. In healthy volunteers, conditioning studies have shown that respiratory symptoms can be influenced by negative expectancies: respiratory symptoms

increase in response to neutral cues that have previously been associated with respiratory symptoms induced by carbon dioxide inhalation (*e.g.* [11, 12]). Accordingly, expectations of respiratory symptoms induced by respiratory loads increase peripheral defensive responses through conditioning [13–15].

A cardinal respiratory symptom in many diseases is dyspnoea, generally defined as the subjective experience of breathing discomfort [16]. The perception of dyspnoea involves sensorimotor, cognitive and emotional aspects that are represented in the processing of induced dyspnoea in the brain. Studies in healthy humans have investigated the neural correlates of dyspnoea by inducing severe respiratory discomfort using resistive loads [17–19] or breath-hold [20] and restricted tidal volume mechanical ventilation [21, 22]. These studies have identified dyspnoea (*i.e.* induced dyspnoea including related emotional and cognitive processes) to be associated with activation in the insula [17, 18, 21–26], the cingulate cortex [22–26] and the periaqueductal gray (PAG) [19, 20, 27]. Furthermore, studies on the neural effects of threatening dyspnoea anticipation additionally implicate the role of the anterior insula, the ventrolateral PAG and the prefrontal cortex (PFC) [19, 28, 29].

Since dyspnoea is a hallmark symptom in a broad range of diseases, worsening of dyspnoea due to expectation can play a critical role in illness perception, progression and treatment. For example, specific triggers (*e.g.* odours, pollutants and allergens) affect asthma exacerbations and symptoms [10, 30]. Subsequently, expecting asthma exacerbations or symptoms to occur based on these specific triggers may lead to actual exacerbations or symptoms in response to the perception of the triggers [10, 11]. Importantly, if expecting dyspnoea not only evokes self-reported dyspnoea and peripheral autonomic reactivity, but also specific brain responses related to dyspnoea processing, this would show that reported worsening of dyspnoea due to expectations is not just a bias in the patients' reporting, but that this bias has a neural basis related to the processing of dyspnoea in the central nervous system.

Consequently, the present study aimed to investigate 1) whether negative expectations can worsen dyspnoea and 2) how this effect is associated with neural processes. In particular, we verbally created the expectation that a specific odorous gas ("Histarinol") would lead to bronchoconstriction and dyspnoea, whereas a control odorous gas would not. In a first phase, the experience phase, this expectation was reinforced by adding a mild resistive load (concealed) into the breathing circuit during the Histarinol condition but not during the control condition. In the second phase, the expectation phase, a very mild resistive load was added in both the Histarinol and the control condition, which allowed us to test for differences in dyspnoea and functional magnetic resonance imaging (fMRI) signal between the Histarinol and control conditions, which were physically identical, but differed with respect to expectation regarding dyspnoea.

Methods

Subjects

36 healthy volunteers completed the study after written consent was obtained (22 females; mean±SD age 25.95±3.29 years). In one volunteer the assessment of blood volume pulse during MR scanning failed, which precluded fMRI noise correction (RETROICOR). Consequently, the sample for the fMRI analysis was comprised of 35 volunteers (22 females; mean±SD age 25.69±2.96 years). The day prior to the experiment, all volunteers underwent medical screening by a physician for eligibility to participate. In particular, normal lung function was determined by a spirometry test (mean±SD forced expiratory volume in 1 s 111.05±12.90% predicted). Volunteers also routinely completed a set of trait questionnaires, assessing anxiety (State-Trait Anxiety Inventory), anxiety sensitivity (Anxiety Sensitivity Index), depression (Beck Depression Inventory), dyspnoea catastrophising (Dyspnoea Catastrophising Scale), social desirability (Social Desirability Scale) and general personality traits (NEO-Five Factor Inventory).

The study protocol was approved by the Ethics Committee of the Chamber of Physicians (Hamburg, Germany) and was conducted at the University Medical Center Hamburg-Eppendorf (Hamburg, Germany).

Breathing system and respiratory measures

Breathing system

Dyspnoea was elicited by breathing through inspiratory flow resistive loads that were introduced into an MR compatible breathing system. Respiratory parameters (tidal volume (V_T), breathing frequency, minute ventilation (V'_E), inspiratory time (T_I), expiratory time (T_E) and end-tidal carbon dioxide tension (P_{ETCO_2})) were continuously recorded using a modified ZAN 600 cardiopulmonary exercise testing device (ZAN Messgeräte, Oberhulba, Germany). A tight-fitting face mask (7450 Series; Hans Rudolph, Shawnee, KS, USA) was attached to the participant's face by means of head gear, to which an elbow tube was connected *via* which odours were nebulised directly in the mask using an olfactometer (figure 1).

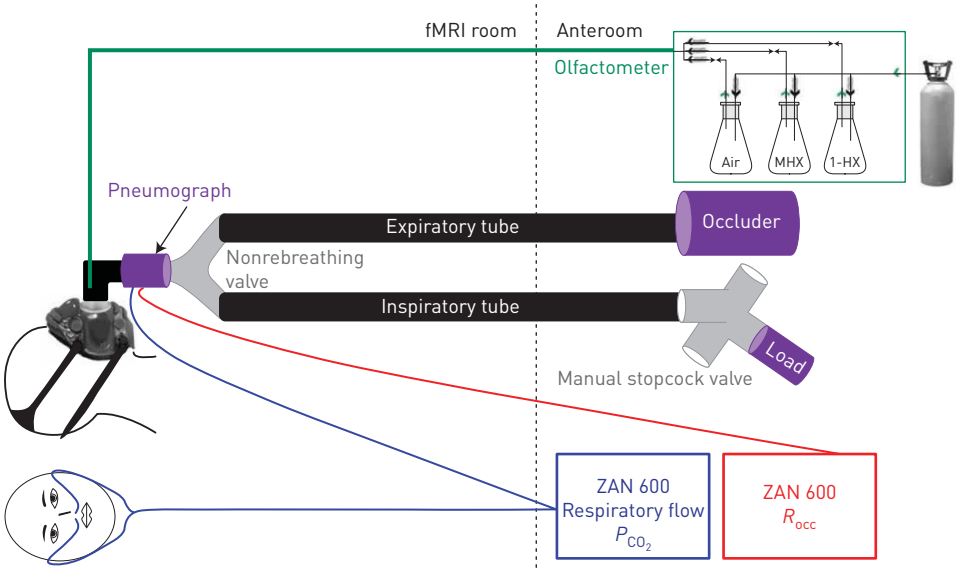

FIGURE 1 Magnetic resonance compatible breathing system. fMRI: functional magnetic resonance imaging; MHX: methylhexanoate; 1-HX: 1-hexanol; P_{CO_2}: carbon dioxide tension; R_{occ}: airway resistance (by occlusion). Volunteers wore an airtight mask connected to a breathing circuit with the possibility of applying loads in the inspiratory pathway. Inside the mask, the respective odours were inserted as nebulised alcohols (or air) *via* an olfactometer. The mask was connected to a respiratory flow sensor (a pneumograph) and end-tidal carbon dioxide tension was sampled *via* a nose cannula, feeding to a ZAN 600 module.

Under the face mask, participants wore a nose cannula to continuously sample P_{ETCO_2}. The elbow tube was connected to the pneumograph to continuously assess respiratory flow. The pneumograph was coupled to a Y-shaped nonrebreathing valve (2630 Series; Hans Rudolph), each end of which was connected to a 10-m tube (inner diameter 1.375 in (~3.5 cm)). At the end of the inspiratory tube, a three-way manual stopcock valve (2110C Series; Hans Rudolph) was attached in order to apply breathing loads of various magnitudes. At the end of the expiratory tube, a shutter valve (ZAN Messgeräte) was attached that allowed an estimation of airway resistance by means of 100-ms occlusions during five consecutive expirations (R_{occ}).

The olfactometer consisted of a custom-built air-proofed polytetrafluoroethylene tube system of 4-mm tubes connecting a gas bottle with compressed air at 6 kPa to three hermetically sealed glass bottles containing either no substance (air), 10 mL 1-hexanol or 10 mL methylhexanoate. Using a system of one-way magnetic valves, tubes derived from each glass bottle merged into one 10-m tube connecting to the elbow piece attached to the face mask. Presentation software (Neurobehavioral Systems, Albany, CA, USA) was used to trigger electrical inductors opening and closing the magnetic valves, in this way nebulising either no odour, 1-hexanol or methylhexanoate with a constant flow.

Dyspnoea ratings

Analogous to previous studies [27], we used a modified Borg rating scale for dyspnoea intensity ratings. We arranged all scale points on a circle, allowing volunteers to select a specific scale point by button presses in either a clockwise and counter-clockwise direction starting from a random scale point. A continuous scale with a random start point from which subjects have to select their level of dyspnoea guarantees that motor activity associated with rating activity and the rating itself are uncorrelated (supplementary figure S1).

Respiratory parameters

All respiratory parameters were continuously assessed during MR scanning. From the continuous carbon dioxide tension and respiratory flow signal, mean P_{ETCO_2} and V'_E were derived during each load and recovery phase. Mean R_{occ} was estimated as the average pressure against 100-ms expiratory occlusions over five consecutive breaths during each load and recovery phase. The respiratory flow signal was unreliable for one participant and R_{occ} measurements were unsuccessful for five participants due to low expiratory flow.

Experimental procedure

On the study day, after providing informed consent, participants were given detailed instructions for the study by the experimenter who wore a white coat signalling their professional status to strengthen the credibility of the instructions. Instructions are available in the supplementary material. These instructions aimed to induce negative expectation effects (*i.e.* nocebo effects) by experience (*i.e.* conditioning) and verbal expectation manipulations. Expectations were manipulated by explaining to participants that they would inhale two different substances, each with a specific odour, of which one would induce dyspnoea, labelled "Histarinol", and the other would not evoke dyspnoea, labelled "Control". Participants were told that both substances were to be administered for 1 min and that their particular odour would fade quickly. Participants were asked to focus on their breathing and breathing sensations throughout the experiment, and to rate dyspnoea intensity when requested. Dyspnoea was specifically described as the increased difficulty and effort to breathe in. Participants were then familiarised with the dyspnoea rating scale. In addition, participants were informed that the long breathing circuit itself would induce minimal dyspnoea, but it was emphasised that the objective was to examine the lasting effects of both substances beyond those of the breathing circuit. Next, the face mask, the respiratory belt and the photoplethysmography sensor to measure blood volume pulse were attached, and the participant was put comfortably in the MR scanner. The respiratory circuit was connected to the face mask and respiratory values were checked before starting the experiment.

The experiment consisted of two parts: an experience phase and an expectation phase. In the first, experience phase, volunteers learned (*i.e.* experienced) that one odorous substance, Histarinol, led to increased dyspnoea, which was not the case for the odorous control substance. Unbeknownst to the volunteers, dyspnoea was induced by applying an inspiratory breathing load (0.81 $kPa \cdot L^{-1} \cdot s^{-1}$). In the second, expectation phase, breathing loads (0.32 $kPa \cdot L^{-1} \cdot s^{-1}$) were identical for the Histarinol and the control condition. The experience and the expectation phase each comprised one Histarinol and one control condition (order counterbalanced), each with eight trials (figure 2). In each trial, a 4-s visual text cue indicated which substance (Histarinol or control) would be applied. Then, one of two odours (1-hexanol or methylhexanoate, counterbalanced) was nebulised for 20 s, so that one odour was paired with dyspnoea and the other was paired with no dyspnoea. The assignment of the two different odours to Histarinol was randomised across subjects. A 50-s load phase started 10 s following odour onset, during which an inspiratory resistive load of 0.81 $kPa \cdot L^{-1} \cdot s^{-1}$ was imposed in the Histarinol trials, whereas no load was imposed in the control trials. The load phase was followed by a 40-s recovery phase. This experience phase allowed volunteers to learn the association between

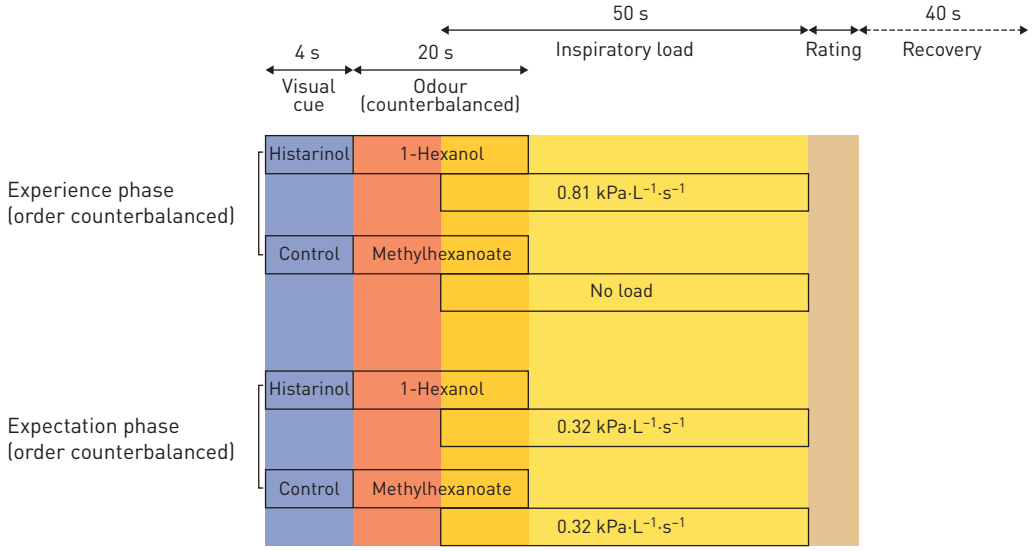

FIGURE 2 Experimental design. The experiment was divided into an experience phase and an expectation phase. In the Histarinol condition of the experience phase, volunteers were exposed to eight trials consisting of a visual cue for 4 s, followed by an odour for 20 s, and 10 s after the odour onset, a 50-s loaded breathing (0.81 $kPa \cdot L^{-1} \cdot s^{-1}$) interval was followed by a rating. In the control condition, volunteers were exposed to eight identical trials, but in this case no load was applied. In the Histarinol and control conditions of the expectation phase volunteers were again exposed to eight trials each; however, in both conditions an identical load (0.32 $kPa \cdot L^{-1} \cdot s^{-1}$) was applied.

a specific visual and/or odorous cue and dyspnoea, and can be seen as the experimental analogue of experience or conditioning, which has been identified as a crucial component in nocebo (and placebo) effects. Importantly, switching between loads always happened during exhalation and thus outside the participant's awareness.

After each load and recovery phase, participants rated dyspnoea intensity on a circular Borg scale ranging from 0 (no noticeable dyspnoea) to 10 (maximally imaginable dyspnoea) (supplementary figure S1). After each session, sensory and affective dyspnoea qualities were assessed by the multidimensional dyspnoea scale. Prior to the start of the study, to provide an anchor point, a load of 3.5 $kPa \cdot L^{-1} \cdot s^{-1}$ was presented for 10 s and participants were instructed that they inhaled a high dose of Histarinol, equivalent to a dyspnoea intensity of 8–9 on the Borg scale. In the subsequent two expectation phases, the same visual and odour cues indicating Histarinol and control trials were both followed by an identical inspiratory load of 0.32 $kPa \cdot L^{-1} \cdot s^{-1}$. At the end of the experiment, the respiratory equipment was removed. The participant left the scanner and was debriefed.

Magnetic resonance scanning

Imaging was performed with a 3-T Siemens MAGNETOM Trio scanner using a 32-channel receive head coil (Siemens Healthcare, Erlangen, Germany). Respiratory parameters and blood volume pulse were measured continuously (Expression; Invivo, Gainesville, FL, USA), digitised (Power 1401-3A; Cambridge Electronic Design, Cambridge, UK) and stored using Spike2 software (Cambridge Electronic Design). Presentation software (Neurobehavioral Systems) was used for stimulus presentation and a CED 1401 analogue–digital converter (Cambridge Electronic Design) was used for response logging. Each of four scanning sessions lasted ~16 min.

Functional magnetic resonance imaging

Blood oxygen level-dependent (BOLD) contrast was measured as an index of local neural activity. 45 axial slices (2 mm thickness, 0.5 mm gap) were acquired by using a gradient echo, echo-planar T2*-sensitive sequence (repetition time (T_R) 2700 ms, echo time (T_E) 25 ms, flip angle 80°, matrix 108×108, field of view 216×216 mm, bandwidth 1544 $Hz \cdot Px^{-1}$). Spatial distortions were reduced by employing parallel acquisition using GRAPPA (generalised autocalibrating partial parallel acquisition) with an acceleration factor of 2 and echo spacing of 0.73 ms.

Structural magnetic resonance imaging

A T1-weighted structural scan (MP RAGE (magnetisation-prepared 180° radiofrequency pulses and rapid gradient echo); T_R 2300 ms, T_E 2.98 ms, flip angle 9°) was acquired. This scan was used for spatial normalisation, registration of functional images and anatomical overlay of brain activations.

Data analysis

Dyspnoea and respiratory variables were analysed using Statistica version 12 (Dell, Austin, TX, USA) and MATLAB version R2018b (MathWorks, Natick, MA, USA).

Dyspnoea and respiratory variables

Dyspnoea intensity ratings and respiratory variables (P_{ETCO_2}, V'_E and R_{occ}) during load phases were submitted to a repeated measures ANOVA with phase (experience *versus* expectation) and condition (Histarinol *versus* control) as within-subject variables. To test for the success of the dyspnoea experience, dyspnoea intensity during loaded breathing (experienced Histarinol) was compared with unloaded breathing (experienced control). To test for expectation-based effects in the context of equal load (*i.e.* nocebo effect), dyspnoea intensity and respiratory variables during expected dyspnoea (expected Histarinol) were compared with the control condition (expected control). Under the hypothesis of an experiential dyspnoea nocebo effect, dyspnoea intensity would be rated higher during expected Histarinol than during expected control, despite inspiratory loads being identical.

Functional brain imaging

Image processing and statistical analyses of images were performed using MATLAB version R2018b and the statistical parametric mapping package SPM12 (www.fil.ion.ucl.ac.uk/spm).

Pre-processing

In a first step all echo-planar imaging (EPI) images of the four sessions (experience: Histarinol, control; expectation: Histarinol, control) were spatially aligned to the first image using a rigid-body transformation (internal smoothing 5 mm full width at half maximum (FWHM), separation 4 mm). In a second step, registered images were averaged and all images were again aligned to the averaged scan. Realigned images

were resliced using a fourth degree B-spline interpolation at the original voxel size. Given the long durations of events, slice timing correction was not performed. The T1-weighted image was co-registered to the mean EPI image using a rigid-body transformation. Parameters were estimated using a mutual information cost function (256×256 intensities joint histogram, 7×7 FWHM smoothing). The co-registered T1 images were then segmented into tissue types and the tissue types were spatially normalised to MNI (Montreal Neurosciences Institute) space using DARTEL. The IXI555 (http://brain-development.org/ixi-dataset) template registered to MNI152 as provided by the CAT12 toolbox (www.neuro.uni-jena.de/cat) was used.

Brainstem-specific pre-processing

Motion correction in SPM employs a 6 degrees of freedom rigid-body transformation model assuming the whole field of view moves consistently. However, given the high degrees of freedom of the atlanto-occipital joint around the *x*-axis ("nodding") these assumptions can be violated (*i.e.* the brainstem moves differently than the cortex). This is particularly problematic for brainstem analyses as the overall parameter estimation for motion parameters is dominated by the cortex given its larger size. However, this can be circumvented by biasing the motion parameter estimation to the brainstem [31]. Therefore, we used a separate pre-processing pipeline using a cylindrical (25 mm radius, length 71 mm) region of interest (ROI) which restricted the spatial pre-processing to brainstem structures (supplementary figure S2).

Single-subject fMRI analysis

Single-subject fMRI analyses were performed in native space; spatial normalisation and smoothing for group-level inference were performed after parameter estimation. For each analysis, a general linear model with the following events was defined: cue, odour, load and rating (for onsets and durations, see figure 2). Each box-car regressor was convolved with a canonical haemodynamic response function as defined by SPM. In addition, we defined nuisance regressors for each session: one block regressor, six realignment movement parameters, one P_{ETCO_2} regressor and 18 physiological parameters as estimated by retrospective image correction RETROICOR using a 3R4C1X scheme [32] which incorporates three cardiac, four respiratory sine and cosine harmonics, and one interaction term (supplementary figure S2 for the effect of noise modelling). The high-pass filter was set to 360 s.

Parameter estimation was performed using a least-squares approach. Parameters were then tested at the single-subject level using appropriate linear contrasts. These contrast images were then spatially normalised using normalisation parameters estimated based on the individual T1-weighted scans and subsequently smoothed with a 6-mm FWHM Gaussian kernel. To account for smaller structures in the brainstem, a smaller smoothing kernel of 2-mm FWHM was chosen for the brainstem data [19].

Linear contrasts tested for differences between Histarinol and control during the experience and expectation phases separately (simple main effects), across both phases (overall main effect) and their difference (phase (experience/expectation)×condition (Histarinol/control) interaction). Analogous to previous studies on nocebo effects in pain [6], we focused our analysis on the load phase of the experiment, but also tested for effects during the other parts in an exploratory fashion.

Group analyses

At the group level, a general linear model was estimated with participant as a random factor. As the contrasts of interest were defined at the single-subject level, a one-sample t-test was performed at the group level. To account for individual relationships with dyspnoea rating, the appropriately contrasted dyspnoea rating was added as a covariate.

The insula is a region consistently associated with dyspnoea [17, 18, 21–26] and was therefore defined as a ROI. We employed one anatomical insula mask of the bilateral insulae (a single ROI comprising all voxels in bilateral insulae) from the three automated anatomical labelling templates (www.gin.cnrs.fr/en/tools/aal). In addition, the midbrain PAG plays a key role in respiratory control in animals (*i.e.* cat/rat) [33, 34] and in humans [19, 27]. Consequently, in the brainstem optimised dataset, we defined the PAG as a ROI, using an anatomical PAG mask as defined in a previous study [19].

Correction for multiple comparisons within ROIs was performed using small volume correction (SVC) based on Gaussian random field theory as implemented in SPM. In the results these corrected p-values are reported as "$p_{(\text{corrected SVC})}$". In addition we also estimated effects for the average of the entire ROI to test whether an effect is represented in the entire structure using MarsBar (http://marsbar.sourceforge.net). For whole-brain analyses, p-values were corrected for multiple comparisons using family-wise error rates and permutation-based (10 000 permutations) threshold free cluster enhancement as implemented in the TFCE

toolbox (www.neuro.uni-jena.de). In the results these corrected p-values are reported as "TFCE" and "p-value corrected". The threshold for statistical significance was set to 0.05.

Results

Dyspnoea ratings and physiological variables

Dyspnoea intensity showed a significant effect of condition (Histarinol *versus* control) ($F(1,35)=19.31$, $p<0.001$, $\eta_p^2=0.36$): dyspnoea intensity was rated significantly higher during Histarinol trials compared with control trials (figure 3a). This was true for both the experience and the expectation phase. Dyspnoea was successfully induced in the experience phase, as shown by higher dyspnoea intensity during experienced Histarinol than experienced control ($F(1,35)=17.09$, $p=0.0002$; mean $\Delta=1.04$, mean experienced control 1.32 (95% CI 0.86–1.78), mean experienced Histarinol 2.36 (95% CI 1.77–2.94)). In addition, a dyspnoea nocebo effect was observed: in the expectation phase, dyspnoea intensity was rated higher during expected Histarinol than during expected control ($F(1,35)=13.04$, $p=0.0009$; mean $\Delta=0.75$, mean expected control 1.35 (95% CI 0.83–1.86), mean expected Histarinol 2.10 (95% CI 1.52–2.68)). The phase×condition interaction for dyspnoea intensity was not significant ($F(1,35)=1.67$, $p=0.21$).

Importantly, these effects cannot be explained by differences in respiratory variables. No significant effects of condition nor significant phase×condition interactions were observed for P_{ETCO_2} ($F(1,35)=0.68$, $p=0.42$; $F(1,35)=0.05$, $p=0.82$) (figure 3b), R_{occ} ($F(1,30)=0.009$, $p=0.92$; $F(1,30)=0.066$, $p=0.80$) (figure 3c) and V'_E ($F(1,34)=0.60$, $p=0.44$; $F(1,34)=0.57$, $p=0.46$) (figure 3d).

Functional brain imaging

Experience phase

In a first analysis we investigated whether an fMRI signal difference related to experienced dyspnoea during Histarinol compared with control could be observed in the experience phase. Our data show a significant signal difference in the left insula (peak *x,y,z*: −39,2,−12 mm, $Z=4.5$, $p=3.4\times10^{-6}$, $p_{(corrected\ SVC)}=0.004$) (figure 4).

Time-courses of the insula show an increased signal during loaded breathing during the experience phase (figure 4c, yellow period). A similar pattern was observed in the contralateral insula, but did not reach our level of significance after correction for multiple comparisons (peak *x,y,z*: 38,14,−2 mm, $Z=3.32$, $p=4.5\times10^{-4}$, $p_{(corrected\ SVC)}=0.21$). Apart from correcting individual activations within bilateral insula, we

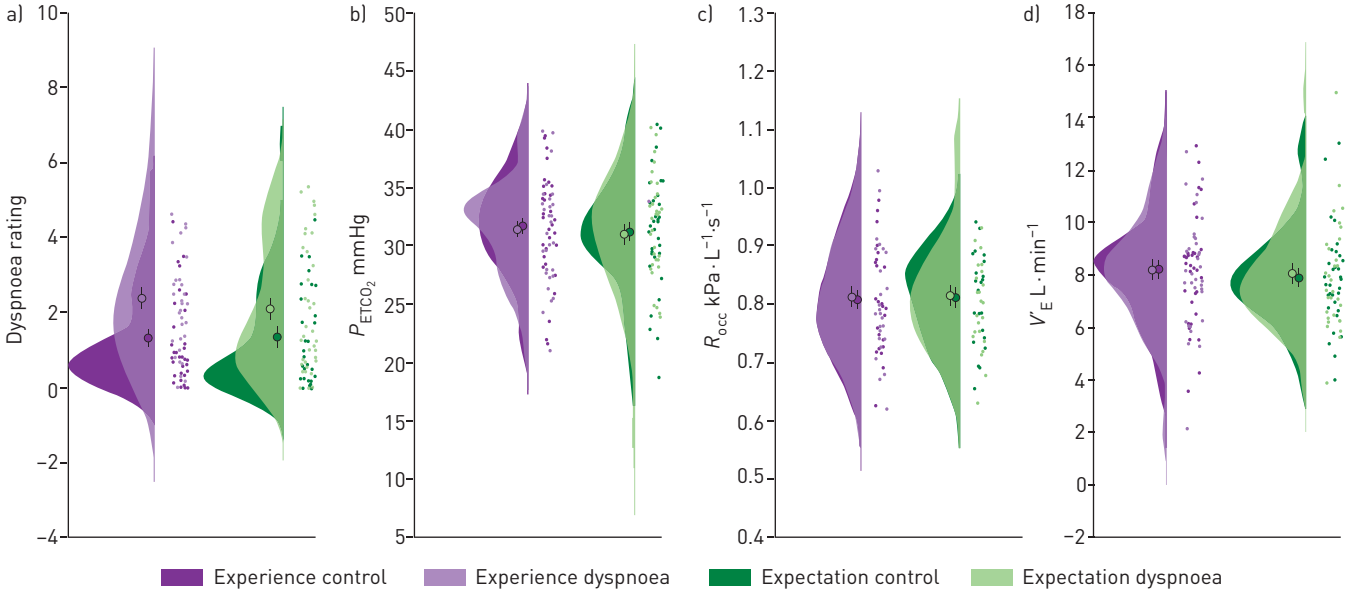

FIGURE 3 Dyspnoea ratings and physiological measurements. P_{ETCO_2}: end-tidal carbon dioxide tension; R_{occ}: airway resistance (by occlusion); V'_E: minute ventilation. a) In the experience phase subjects rated subjective dyspnoea in the loaded breathing (Histarinol) condition higher than in the control condition. Importantly, the same difference was seen in the expectation phase although the respiratory load in the Histarinol and control conditions was identical. b–d) No significant differences were observed for b) P_{ETCO_2}, c) R_{occ} and d) V'_E. Dots represent individual data and "clouds" depict estimated data distribution. Circles and lines represent mean±SEM.

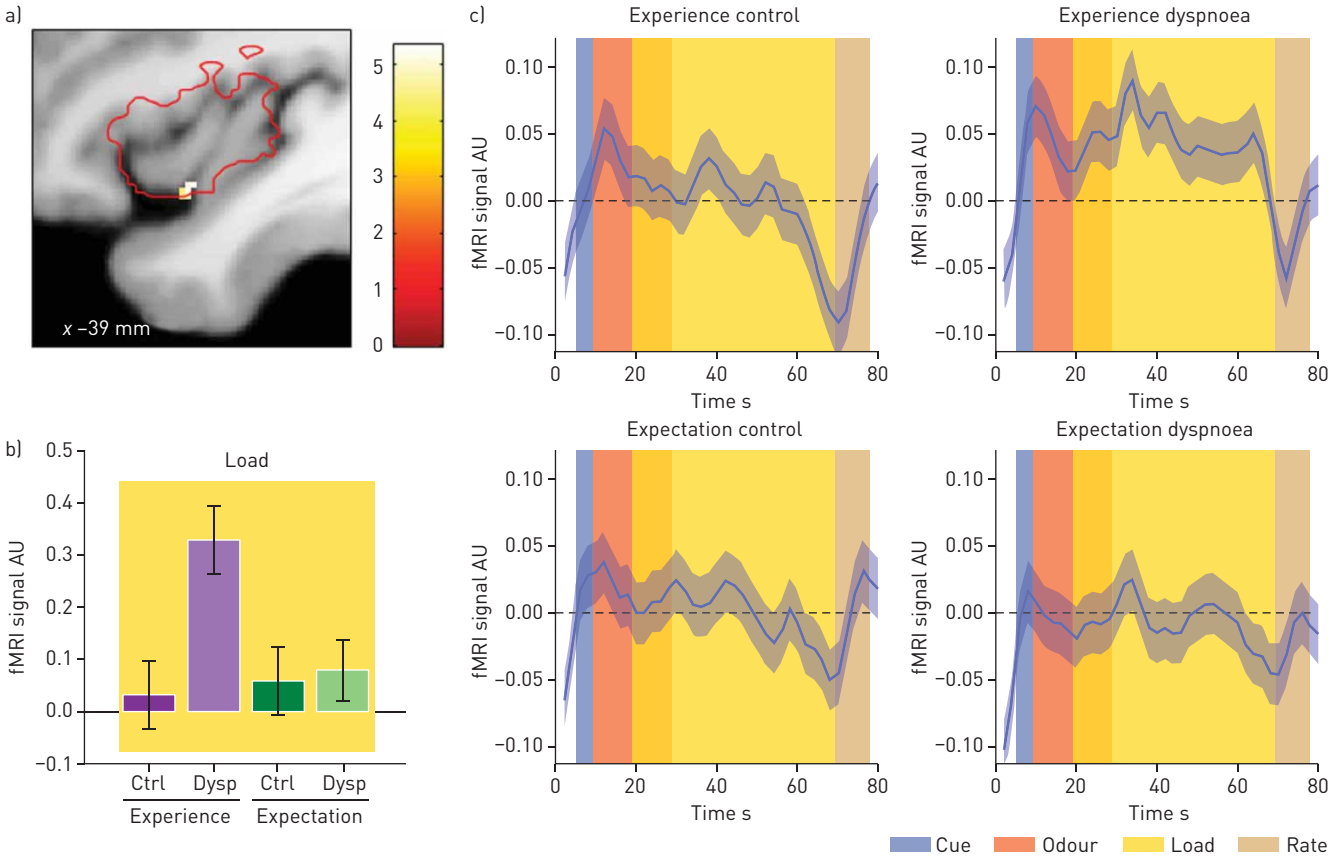

FIGURE 4 Functional magnetic resonance imaging (fMRI) signal differences in the experience phase between experienced dyspnoea (Histarinol) and control within the insula region of interest (ROI). AU: arbitrary units. a) Location of the activation cluster overlaid on the average T_1-weighted image and thresholded at p<0.05 (corrected). Insula ROI depicted as red contour. b) Bar graphs (mean±SEM) depict activation for both phases (experience and expectation) and conditions (control ("Ctrl") and Histarinol ("Dysp")) during loaded breathing. c) Smoothed (Gaussian full width at half maximum 4 s) activation time-courses (mean±SEM) averaged across trials. The colour bars are shifted to the right by 5 s to account for the delay of the haemodynamic response function.

investigated whether the insula as a whole shows a similar signal pattern. The signal averaged across bilateral insula again revealed a significant effect ($t(33)=2.27$, p=0.015) for the experience phase, showing a significantly higher fMRI signal during the experience of dyspnoea compared with the control condition.

Expectation phase

In a second step we compared the dyspnoea (Histarinol) condition to the control condition in the expectation phase, in which the breathing resistance was identical for both conditions. Analyses focusing on the insula revealed no significant difference during dyspnoea expectation (Histarinol) to control. However, whole-brain analyses corrected for multiple comparisons using nonparametric TFCE showed a significant activation in the dorsomedial PFC (peak *x,y,z*: −17,36,47 mm, TFCE=2347, p=0.007 corrected) (figure 5; for a whole-brain panel, see supplementary figure S3). Here we observed a strong difference between the dyspnoea (Histarinol) and the control condition, with a reduction of the fMRI signal in the Histarinol condition and an increase in the control condition.

A similar activation pattern was observed in the rostral anterior cingulate cortex (rACC) (rACC and ventromedial PFC are used interchangeably in this article) (peak *x,y,z*: −6,62,2 mm, TFCE=2026, p=0.014 corrected; peak *x,y,z*: −6,50,−12 mm; TFCE=1982, p=0.016 corrected) and the posterior cingulate cortex (PCC) (peak *x,y,z*: −9,−56,36 mm, TFCE=2086, p=0.013 corrected) (figure 6; for a whole-brain panel, see supplementary figure S3).

Since separate analyses for the experience and expectation phases of the experiment do not allow statements regarding specificity of the effects for either phase, we additionally tested a phase×condition interaction, available in the supplementary material.

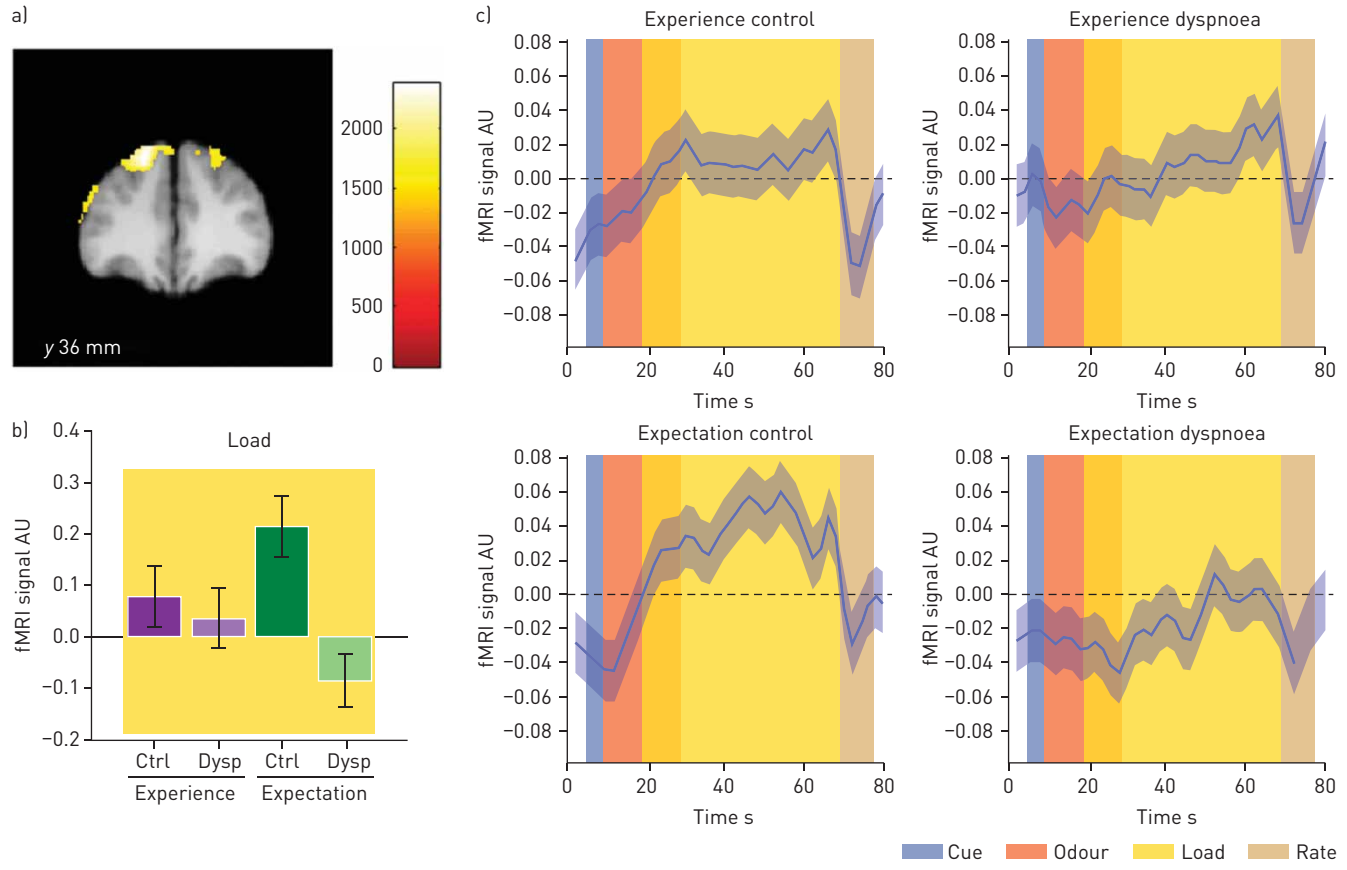

FIGURE 5 Functional magnetic resonance imaging (fMRI) signal differences in the expectation phase between expected dyspnoea (Histarinol) and control in the dorsomedial prefrontal cortex. AU: arbitrary units. a) Location of the activation cluster overlaid on the average T_1-weighted image and thresholded at p<0.05 (corrected). b) Bar graphs (mean±SEM) depict activation for both phases (experience and expectation) and conditions (control ("Ctrl") and Histarinol ("Dysp")) during loaded breathing. c) Smoothed (Gaussian full width at half maximum 4 s) activation time-courses (mean±SEM) averaged across trials. The colour bars are shifted to the right by 5 s to account for the delay of the haemodynamic response function.

Association with self-reports

We also wanted to link patterns of activation to individual self-reports. We therefore performed additional fMRI analyses in which we correlated the rating differences between control and dyspnoea for both phases (separately for the experience and expectation phases). Here we observed a relationship between rating differences and fMRI signal changes in the precuneus and PCC (peak *x*,*y*,*z*: 3,−56,41 mm, TFCE=2214, p=0.002 corrected) (figure 7) for the expectation phase only. Importantly, the peak of this correlation was located within the main effect comparing the Histarinol condition with the control condition during the expectation phase (supplementary figure S6).

Brainstem

Finally, we investigated BOLD responses in a brainstem optimised dataset, with a particular focus on the PAG [19, 20, 27]. This analysis revealed a main effect of Histarinol across the experience and the expectation phase in the caudal dorsomedial PAG (peak *x*,*y*,*z*: 2,−36,−14 mm, *Z*=3.7, $p=9.3\times10^{-5}$, $p_{(corrected\ SVC)}=0.027$) (figure 8; for an unmasked activation map at p<0.001, see supplementary figure S7). In addition, a simple main effect during the expectation phase with higher signal for the expected dyspnoea (Histarinol) condition was observed in the dorsolateral PAG (peak *x*,*y*,*z*: −3,−38,−12 mm, *Z*=3.9, $p=5.6\times10^{-5}$, $p_{(corrected\ SVC)}=0.016$). The time-course of the dorsomedial PAG depicted in figure 8c also suggests stronger activation during the cue phase for the Histarinol compared with the control condition. However, this effect was not significant (peak *x*,*y*,*z*: 2,−38,−11 mm, *Z*=3.4, $p=2.9\times10^{-4}$, $p_{(corrected\ SVC)}=0.07$). Apart from correcting individual activations within the PAG, we investigated whether the PAG as a whole shows a similar signal pattern. The signal averaged across all voxels in the PAG revealed no significant effect for either the overall main effect across both phases ($t(33)=1.13$, p=0.13) or the simple main effect during the expectation phase ($t(33)=1.5$, p=0.07), suggesting a focal effect constrained to the caudal part of the PAG (figure 8).

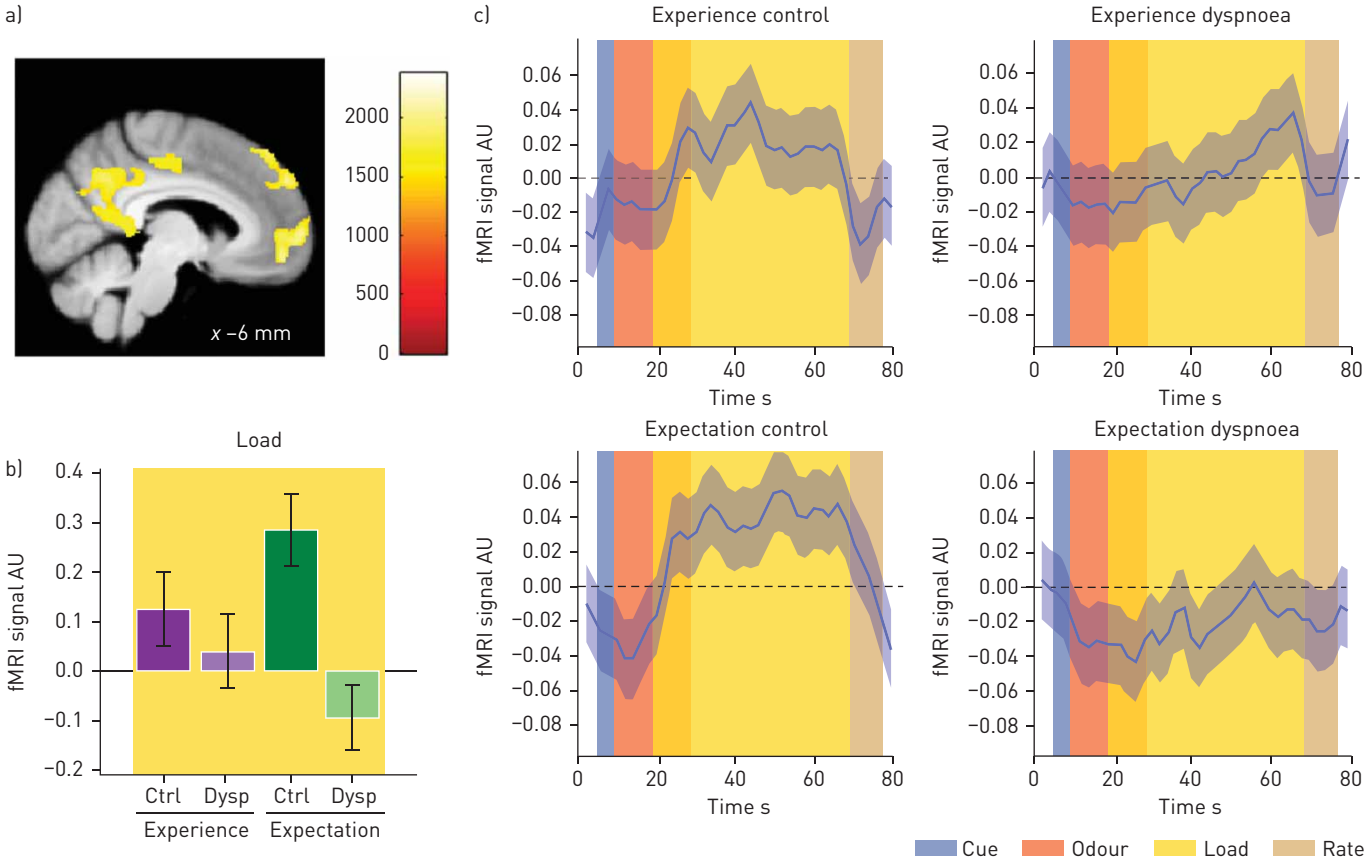

FIGURE 6 Functional magnetic resonance imaging (fMRI) signal differences in the expectation phase between expected dyspnoea (Histarinol) and control in the rostral anterior cingulate cortex. a) Location of the activation cluster overlaid on the average T_1-weighted image and thresholded at p<0.05 (corrected). b) Bar graphs (mean±SEM) depict activation for both phases (experience and expectation) and conditions (control ("Ctrl") and Histarinol ("Dysp")) during loaded breathing. c) Smoothed (Gaussian full width at half maximum 4 s) activation time-courses (mean±SEM) averaged across trials. The colour bars are shifted to the right by 5 s to account for the delay of the haemodynamic response function.

Analyses regarding fMRI signal differences during the cue or the odour part of each trial revealed no significant differences.

Discussion

Our data clearly show that the mere expectation of dyspnoea triggered by an odour can lead to experienced dyspnoea. This subjective difference was observed in the absence of changes in physiological variables including ventilation and airway resistance. For the dyspnoea condition (Histarinol) the insula showed an increased fMRI signal, mirroring actual physical stimulus properties (*i.e.* resistive load). In contrast, BOLD responses in the PAG showed a significant dyspnoea-related signal in the expectation phase. In addition, we observed a dyspnoea-related deactivation in the dorsomedial PFC, rACC and PCC during the expectation phase. Signal differences in the PCC were correlated with individual rating differences during this expectation phase.

Using a brainstem optimised pre-processing procedure [31], our data revealed an increased fMRI signal during the Histarinol condition compared with the control condition in the caudal PAG during the expectation phase. Similar responses were observed during the experience phase. This pattern closely resembles the perceived dyspnoea, which shows similarly high ratings for the Histarinol condition in both the experience and the expectation phase (figures 3 and 8). Using a small smoothing kernel of 2 mm, we could localise the PAG activation to the caudal part of the dorsolateral PAG and dorsomedial PAG. The activation in the dorsolateral PAG is in agreement with rodent studies indicating a role of the dorsolateral PAG in active breathing and increased respiratory effort [33, 34]. Previously, fMRI studies have mainly observed and characterised BOLD signal changes in the caudal lateral and ventrolateral [19, 20] or rostral PAG [27]. In a conditioned respiratory threat study [19], a deactivation during loaded breathing in the lateral PAG was

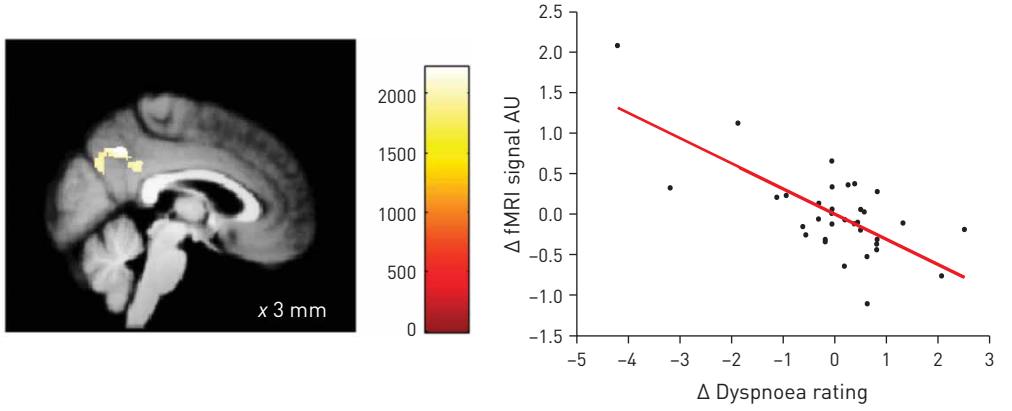

FIGURE 7 Functional magnetic resonance imaging (fMRI) signal differences in the expectation phase are correlated with rating differences between expected dyspnoea and expected dyspnoea (Histarinol) in the posterior cingulate cortex ($p<0.05$ corrected TFCE). AU: arbitrary units.

observed. This deactivation was located rostral from ours ($z=-8$ mm), also replicating previous findings from the same group showing a similar deactivation for breath-hold in the lateral PAG [20]. During the anticipation of load, the authors observed an activation in the ventrolateral PAG at $z=-13$ mm. However, no activation differences in the dorsolateral or dorsomedial part of the PAG were observed.

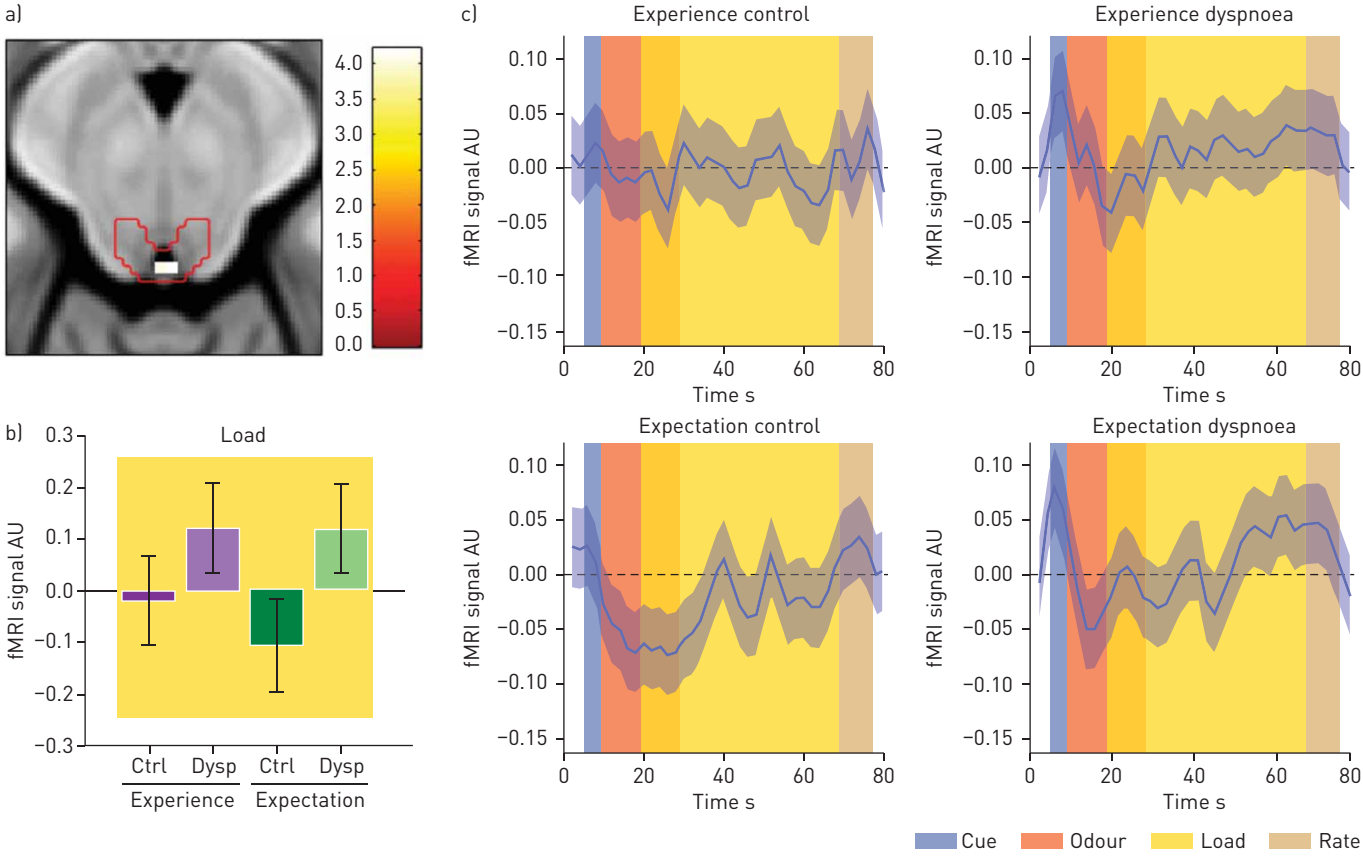

FIGURE 8 Main effect for Histarinol *versus* control within the periaqueductal gray (PAG) region of interest across the experience and expectation phase. a) Location of the activation cluster within the PAG mask (red contour) overlaid on an anatomical template and thresholded at $p<0.05$ (corrected). b) Bar graphs (mean±SEM) depict activation for both phases (experience and expectation) and conditions (control ("Ctrl") and Histarinol ("Dysp")) during loaded breathing. c) Smoothed (Gaussian full width at half maximum 4 s) activation time-courses (mean±SEM) averaged across trials. The colour bars are shifted to the right by 5 s to account for the delay of the haemodynamic response function.

We also observed a dyspnoea-related deactivation in the rACC, which has been implicated repeatedly in expectation effects regarding pain. Initially, this structure was exclusively linked with placebo analgesia [31, 35, 36], showing increased fMRI signals in the rACC during positive treatment expectation, *i.e.* the placebo condition. In a placebo analgesia study with an explicit value component (*i.e.* cheap and expensive placebo), activation in the rACC during the placebo condition was positively correlated with treatment value [36]. However, recently this structure was also implicated in negative treatment value in the context of pain, *i.e.* nocebo hyperalgesia [6], in a study which contained an explicit treatment value component (*i.e.* cheap and expensive treatment) and revealed that the rACC showed a decrease in activation during the nocebo condition and that this decrease was correlated with the magnitude of the nocebo effect. Taken together, for placebo hypoalgesia the rACC shows an activation, whereas for nocebo hyperalgesia the rACC shows a deactivation. Previously, areas in the medial part of the PFC such as the rACC/ventromedial PFC have been shown to encode (economic) value for a variety of objects, including small items, money and food [37, 38]. Integrating these observations with placebo and nocebo studies has led to the notion that this part of the ventromedial PFC also encodes treatment value [6]. The data from the present study support this notion, by showing a reduced fMRI signal in the expectation dyspnoea condition during the load interval, which is associated with a negative (aversive) value as acquired in the preceding experience part of the experiment. Our results therefore extend treatment value results from the pain domain [6] to the respiratory domain. This interpretation is further supported by a deactivation of the dorsomedial PFC, which has also been linked to subjective value [39], during the respiratory nocebo condition.

In the expectation phase, we observed a correlation between the rating differences for control and Histarinol and fMRI signal changes in the PCC. An early positron emission tomography (PET) study using resistive loads during inspiration and expiration revealed a positive correlation between brain activity in the PCC and intensity/unpleasantness of induced dyspnoea [17]. This seems to be at odds with our data showing such a correlation in the expectation phase. However, in this PET study, activation in the PCC was specifically associated with subjective dyspnoea, but unrelated to the respiratory motor response, and thus the physical induction of dyspnoea. This can explain why such a correlation can also be observed in our expectation phase. However, we currently cannot explain why we did not observe such a correlation during the experience phase. This might be related to substantial differences between both studies (*e.g.* fMRI *versus* PET and load intensity).

In sum, dyspnoea expectations specifically signalled by visual and/or odour cues can enhance the intensity of the symptom, both in self-reports [10, 30] and neural activation [19]. In asthma particularly, odours are critical triggers of asthma exacerbations and thus merely expecting asthma worsening based on perceived odours could trigger asthma symptoms or exacerbations [10, 30]. These expectations can derive from unconscious processes leading to automatic responses, as would be the case in classical conditioning resulting from repeated associations between asthma triggers and symptoms, such as the pairing of an odour and dyspnoea in the current paradigm, or from conscious processes, such as conscious learning during classical conditioning or verbal instructions as given in the current study. Furthermore, expectancy-driven neural activation associated with dyspnoea and respiratory effort in response to odours may strengthen the odour–symptom association, and in this way enhance the perception of asthma symptoms. In addition, expectations of asthma symptoms based on odour cues may not only increase perception and neural activation of dyspnoea, but, conversely, perception and neural activation of dyspnoea in response to odours may enhance expectations of asthma symptoms, resulting in a vicious cycle reinforcing dyspnoea and expectations of dyspnoea [2]. Moreover, if the learned associations between odours and asthma symptoms generalise to related triggers, this may further enhance asthma symptoms. Likewise, asthma symptoms may not only increase by classical conditioning, but also instrumental learning may play a role; when experiencing asthma symptoms in response to asthma triggers, coping behaviours are initiated that will relieve symptoms. This relief of symptoms resulting from coping behaviours in response to expectation-based symptoms may further reinforce the associations between specific asthma triggers, symptoms, coping responses and relief of symptoms, strengthening the vicious cycle of dyspnoea expectation and perception.

Finally, predictive coding models argue that expectations may dominate perception especially when sensations are vague, which may lead to an exaggerated perception of dyspnoea and a poor correspondence between dyspnoea perceptions and objective dyspnoea sensations [2]. These dyspnoea-enhancing processes, which require further investigation, are particularly important since, in respiratory disease, experienced dyspnoea shows a stronger association with mortality than actual lung function [40]. Moreover, since dyspnoea is not only a key symptom in respiratory disease, but also in cardiovascular disease, anxiety disorders, post-operative states and illness in general [16], contextual factors of settings in which dyspnoea occurs, and expectations associated with these, may have widespread implications for symptom perception in a variety of diseases.

Despite important new insights resulting from this study, some limitations need to be acknowledged. First, the respiratory loads used in the present study were mild and thus some caution is required when generalising the implications of the present findings to nocebo effects of severe dyspnoea symptoms. Second, future research should investigate the importance of nocebo dyspnoea in patient groups with adjusted experimental designs, since patients, compared with healthy volunteers, may show altered sensitivity to respiratory sensations and interoceptive accuracy, and have already well-established, and potentially generalised, associations between specific triggers and dyspnoea [2]. Third, the nocebo effects in this study are limited to dyspnoea induced by inspiratory resistive loads, targeting respiratory effort. Additional future research perspectives include studying neural expectation effects of dyspnoea dimensions other than breathing effort, such as air hunger and chest tightness, as well as triggers other than odours. Fourth, it would be interesting to directly investigate the role of experience (*i.e.* learning) using a time×condition interaction. However, in our case such an analysis is potentially confounded by the fact that the control and the Histarinol runs were performed sequentially. Future studies could interleave Histarinol and control trials within the experience and the expectation phase, which would allow for an unconfounded condition×time interaction analysis. Furthermore, future research could examine the neural correlates of generalisation, higher-order conditioning and instrumental learning of dyspnoea to investigate their role in the dyspnoea perception process of patients. Finally, the present findings suggest that research designs similar to the current design can be used to explore the neural mechanisms of dyspnoea-related placebo effects.

In summary, this study illustrates that mere expectations can enhance the experienced intensity and the neural processing of dyspnoea or respiratory effort. In this way, expectations may create, maintain and strengthen associations between dyspnoea and dyspnoea triggers, both experientially and neurally, critically affecting perception, progression and treatment of respiratory symptoms. Our findings help understand expectation related activity in experimental dyspnoea in healthy volunteers. Appropriate translational research is now necessary to contextualise these findings in patient populations.

Acknowledgements: We would like to thank the radiographer and physics team at the Dept for Systems Neuroscience (University Medical Center Hamburg-Eppendorf, Hamburg, Germany) for help with scanning. We also would like to thank Olivia Harrison (née Faull) (University of Otago, Dunedin, New Zealand) for providing the anatomical PAG mask.

Conflict of interest: E. Vlemincx reports grants from the European Research Council (ERC-2010-AdG_20100407), during the conduct of the study. C. Sprenger reports grants from the European Research Council (ERC-2010-AdG_20100407), during the conduct of the study. C. Büchel reports grants from the European Research Council (ERC-2010-AdG_20100407), during the conduct of the study.

Support statement: C. Büchel is supported by the German Research Foundation (DFG; SFB 289 project A02). E. Vlemincx, C. Büchel and C. Sprenger were supported by the European Research Council (ERC-2010-AdG_20100407). Funding information for this article has been deposited with the Crossref Funder Registry.

References

1 Büchel C, Geuter S, Sprenger C, *et al.* Placebo analgesia: a predictive coding perspective. *Neuron* 2014; 81: 1223–1239.
2 Van den Bergh O, Witthöft M, Petersen S, *et al.* Symptoms and the body: taking the inferential leap. *Neurosci Biobehav Rev* 2017; 74: 185–203.
3 Ongaro G, Kaptchuk TJ. Symptom perception, placebo effects, and the Bayesian brain. *Pain* 2019; 160: 1–4.
4 Atlas LY, Wager TD. A meta-analysis of brain mechanisms of placebo analgesia: consistent findings and unanswered questions. *Handb Exp Pharmacol* 2014; 225: 37–69.
5 Petersen GL, Finnerup NB, Colloca L, *et al.* The magnitude of nocebo effects in pain: a meta-analysis. *Pain* 2014; 155: 1426–1434.
6 Tinnermann A, Geuter S, Sprenger C, *et al.* Interactions between brain and spinal cord mediate value effects in nocebo hyperalgesia. *Science* 2017; 358: 105–108.
7 Wechsler ME, Kelley JM, Boyd IOE, *et al.* Active albuterol or placebo, sham acupuncture, or no intervention in asthma. *N Engl J Med* 2011; 365: 119–126.
8 Wolters F, Peerdeman KJ, Evers AWM. Placebo and nocebo effects across symptoms: from pain to fatigue, dyspnea, nausea, and itch. *Front Psychiatry* 2019; 10: 470.
9 Wise RA, Bartlett SJ, Brown ED, *et al.* Randomised trial of the effect of drug presentation on asthma outcomes: the American Lung Association Asthma Clinical Research Centers. *J Allergy Clin Immunol* 2009; 124: 436–444.
10 Jaén C, Dalton P. Asthma and odors: the role of risk perception in asthma exacerbation. *J Psychosom Res* 2014; 77: 302–308.

11 Peuter SD, Diest IV, Lemaigre V, *et al.* Can subjective asthma symptoms be learned? *Psychosom Med* 2005; 67: 454–461.
12 Van den Bergh O, Stegen K, Van Diest I, *et al.* Acquisition and extinction of somatic symptoms in response to odours: a Pavlovian paradigm relevant to multiple chemical sensitivity. *Occup Environ Med* 1999; 56: 295–301.
13 Pappens M, Van den Bergh O, Vansteenwegen D, *et al.* Learning to fear obstructed breathing: comparing interoceptive and exteroceptive cues. *Biol Psychol* 2013; 92: 36–42.
14 Benke C, Alius MG, Hamm AO, *et al.* Cue and context conditioning to respiratory threat: effects of suffocation fear and implications for the etiology of panic disorder. *Int J Psychophysiol* 2018; 124: 33–42.
15 Lang PJ, Wangelin BC, Bradley MM, *et al.* Threat of suffocation and defensive reflex activation. *Psychophysiology* 2011; 48: 393–396.
16 Parshall MB, Schwartzstein RM, Adams L, *et al.* An Official American Thoracic Society Statement: update on the mechanisms, assessment, and management of dyspnea. *Am J Respir Crit Care Med* 2012; 185: 435–452.
17 Peiffer C, Poline J-B, Thivard L, *et al.* Neural substrates for the perception of acutely induced dyspnea. *Am J Respir Crit Care Med* 2001; 163: 951–957.
18 von Leupoldt A, Sommer T, Kegat S, *et al.* The unpleasantness of perceived dyspnea is processed in the anterior insula and amygdala. *Am J Respir Crit Care Med* 2008; 177: 1026–1032.
19 Faull OK, Jenkinson M, Ezra M, *et al.* Conditioned respiratory threat in the subdivisions of the human periaqueductal gray. *eLife* 2016; 5: e12047.
20 Faull OK, Jenkinson M, Clare S, *et al.* Functional subdivision of the human periaqueductal grey in respiratory control using 7 tesla fMRI. *NeuroImage* 2015; 113: 356–364.
21 Banzett RB, Mulnier HE, Murphy K, *et al.* Breathlessness in humans activates insular cortex. *Neuroreport* 2000; 11: 2117–2120.
22 Evans KC, Banzett RB, Adams L, *et al.* BOLD fMRI identifies limbic, paralimbic, and cerebellar activation during air hunger. *J Neurophysiol* 2002; 88: 1500–1511.
23 Binks AP, Evans KC, Reed JD, *et al.* The time-course of cortico-limbic neural responses to air hunger. *Respir Physiol Neurobiol* 2014; 204: 78–85.
24 Brannan S, Liotti M, Egan G, *et al.* Neuroimaging of cerebral activations and deactivations associated with hypercapnia and hunger for air. *Proc Natl Acad Sci USA* 2001; 98: 2029–2034.
25 Corfield DR, Fink GR, Ramsay SC, *et al.* Evidence for limbic system activation during CO_2-stimulated breathing in man. *J Physiol* 1995; 488: 77–84.
26 Liotti M, Brannan S, Egan G, *et al.* Brain responses associated with consciousness of breathlessness (air hunger). *Proc Natl Acad Sci USA* 2001; 98: 2035–2040.
27 von Leupoldt A, Sommer T, Kegat S, *et al.* Down-regulation of insular cortex responses to dyspnea and pain in asthma. *Am J Respir Crit Care Med* 2009; 180: 232–238.
28 Hayen A, Wanigasekera V, Faull OK, *et al.* Opioid suppression of conditioned anticipatory brain responses to breathlessness. *Neuroimage* 2017; 150: 383–394.
29 Nakai H, Tsujimoto K, Fuchigami T, *et al.* Effect of anticipation triggered by a prior dyspnea experience on brain activity. *J Phys Ther Sci* 2015; 27: 635–639.
30 Isenberg SA, Lehrer PM, Hochron S. The effects of suggestion on airways of asthmatic subjects breathing room air as a suggested bronchoconstrictor and bronchodilator. *J Psychosom Res* 1992; 36: 769–776.
31 Eippert F, Bingel U, Schoell ED, *et al.* Activation of the opioidergic descending pain control system underlies placebo analgesia. *Neuron* 2009; 63: 533–543.
32 Harvey AK, Pattinson KTS, Brooks JCW, *et al.* Brainstem functional magnetic resonance imaging: disentangling signal from physiological noise. *J Magn Reson Imaging* 2008; 28: 1337–1344.
33 Bandler R, Depaulis A. Midbrain periaqueductal gray control of defensive behavior in the cat and the rat. *In*: Depaulis A, Bandler R, eds. The Midbrain Periaqueductal Gray Matter: Functional, Anatomical, and Neurochemical Organisation. Boston, Springer, 1991; pp. 175–198.
34 Subramanian HH, Balnave RJ, Holstege G. The midbrain periaqueductal gray control of respiration. *J Neurosci* 2008; 28: 12274–12283.
35 Bingel U, Lorenz J, Schoell E, *et al.* Mechanisms of placebo analgesia: rACC recruitment of a subcortical antinociceptive network. *Pain* 2006; 120: 8–15.
36 Geuter S, Eippert F, Hindi Attar C, *et al.* Cortical and subcortical responses to high and low effective placebo treatments. *Neuroimage* 2013; 67: 227–236.
37 Gottfried JA, O'Doherty J, Dolan RJ. Encoding predictive reward value in human amygdala and orbitofrontal cortex. *Science* 2003; 301: 1104–1107.
38 Lebreton M, Jorge S, Michel V, *et al.* An automatic valuation system in the human brain: evidence from functional neuroimaging. *Neuron* 2009; 64: 431–439.
39 Piva M, Velnoskey K, Jia R, *et al.* The dorsomedial prefrontal cortex computes task-invariant relative subjective value for self and other. *eLife* 2019; 8: e44939.
40 Nishimura K, Izumi T, Tsukino M, *et al.* Dyspnea is a better predictor of 5-year survival than airway obstruction in patients with COPD. *Chest* 2002; 121: 1434–1440.